Available online at www.sciencedirect.com
ScienceDirect
Journal of Power Sources 179 (2008) 451–457
JOURNAL OF POWER SOURCES
www.elsevier.com/locate/jpowsour

Determination of bidirectional permeability of proton exchange membranes using a ^{1}H nuclear magnetic resonance technique

Eun Ah Kim [a], Tae Kyoung Kim [b], Chanho Pak [a], Hyuk Chang [a], Doyoung Seung [a], Yeong Suk Choi [a,*]

[a] *Energy & Environment Laboratory, Samsung Advanced Institute of Technology (SAIT), P.O. Box 111, Suwon 449-600, Republic of Korea*
[b] *Research Institute of Chemical & Electronic Materials, Cheil Industries Inc., Uiwang-si 437-711, Republic of Korea*

Received 21 September 2007; received in revised form 19 October 2007; accepted 7 January 2008
Available online 30 January 2008

Abstract

Bidirectional permeability of proton exchange membranes was measured using a ^{1}H nuclear magnetic resonance (NMR) technique based on the assignment of characteristic peaks and derivation of a relationship between the peak areas and the concentrations of methanol, water and D_2O. The concentration variations of the liquids determined with NMR spectra showed that both methanol and the water transports were affected by the thickness and the chemical structure of membranes. Molar ratios of methanol to water diffused through membranes elucidated that chemical structures of membranes had a strong influence on the methanol transport, compared to thickness. Reverse-direction diffusion behaviors of membranes, back-diffusions, were also appraised with the D_2O amounts. The amounts of back-diffusions were much less than those of the water transported from the opposite direction, which is the first report on the direct measurements of back-diffusions. The results suggest that ^{1}H NMR technique can evaluate bidirectional transports of proton exchange membranes.

Keywords: Proton exchange membranes; Permeability; Back-diffusion; ^{1}H nuclear magnetic resonance; Transport behavior

1. Introduction

Recently, fuel cells are attracting much attention in science and engineering fields because of high efficiency in energy conversion and low emission of greenhouse gas, compared to fossil fuels. Direct methanol fuel cell (DMFC) is considered as a power source for portable electronic devices due to its high power density and convenience of refilling fuels [1,2].

Efficiencies of DMFC systems relate to cell voltages which are affected by decreases in open circuit voltages (OCVs), activation losses, ohmic resistance losses and mass transfer losses; decreases in OCVs result from reverse potentials of cathodes induced by the methanol diffused from anodes. Activation losses involve voltage decreases by the slow activation of anode catalysts. Ohmic resistance losses engage in voltage decreases by the ionic resistances of proton exchange membranes (PEMs) through which protons transport from anodes to cathodes through ion channels. Fuel depletions or byproduct accumulations within catalyst layers contribute to mass transport losses [3]. As briefly summarized, most of the voltage decreases except the decreases by the activation losses are correlated with transport behaviors or permeability of PEMs [4]. Consequently, permeability among various properties becomes important in the developments and evaluations of PEMs.

PEMs of DMFCs have fluxes in, at least, two directions: (1) transports from anodes to cathodes, (2) reverse-direction transports from cathodes to anodes [5–10]. The former (methanol and water transports) can be measured by using spectroscopic techniques: gas chromatography (GC) and reflective index (RI) methods [11]. The latter (back-diffused water transports), however, is not measurable, because the water transported reversely from cathodes is not discernible from the anodic water [12,13]. Since full-passive DMFCs operate without active fuel-

* Corresponding author. Tel.: +82 31 280 9326; fax: +82 31 280 9359.
E-mail address: Yeongsuk.choi@samsung.com (Y.S. Choi).

0378-7753/$ – see front matter © 2008 Elsevier B.V. All rights reserved.
doi:10.1016/j.jpowsour.2008.01.033

feeding devices, such as pumps for methanol feeding and air compressors (or fans) for air feeding, the cell performances of full-passive DMFCs largely rely on water and air managements [14]. The reverse water transport is one of the critical factors for the water management and the cell performances of full-passive DMFCs. Therefore, comprehending bidirectional transports through PEMs is pivotal for the commercialization of DMFCs. Due to the technical limit to the measurement of reverse-direction water transports, the studies on bidirectional transports have been rarely reported yet. So a new method for measuring bidirectional diffusions through PEMs is required.

^{1}H NMR is a well-known tool for not only identifying chemical species but also determining their concentrations. Logically, provided that ^{1}H NMR spectra of designated species are not overlapped, we can estimate the concentrations of the species.

In this paper, a new method for determining bi-directional permeabilities of PEMs was developed using an NMR technique. Transport behaviors of perfluorinated membranes (Nafion) and a commercial hydrocarbon membrane were also elucidated [15,16]. To utilize ^{1}H NMR technique for the measurement of bidirectional permeability, we had to set up relations between peak intensities of ^{1}H NMR spectra and concentrations of chemical species. Deuterium oxide (D_2O) was adopted for the cathodic water, because its molecular size is similar to that of water and the diffused materials have discrete characteristic peaks in ^{1}H NMR spectra.

From an application point of view, Nafion membranes are reported to have high degree of methanol crossover and water transport, which cause reverse potential and water flooding in cathodes, leading to the decrease in DMFC cell performances. Consequently, new proton exchange membranes are required to overcome the shortcoming of Nafion membranes. Furthermore, the actual comparison of Nafion and hydrocarbon-based PEMs in bidirectional transports has not been reported yet. This work exhibited methanol and water transports, molar ratios of methanol to water transported through membranes and, finally, reverse-direction water transport behaviors of membranes.

2. Experimental

2.1. Materials

The water used for this experiment was deionized water with a resistivity of 18.2 MΩ cm at 25 °C, which was prepared using a Mili-Q water purification system from Milipore Com. Deuterated dimethyl sulfoxide (DMSO-d_6) and deuterium oxide, purchased from Aldrich, were used for the NMR solvent and the diffusion solvent (cathodic water), respectively. High-purity pyridine (C_5H_5N), purchased from Aldrich, was used as the external standard for estimating concentrations of methanol, water and D_2O.

The membranes for permeability measurements were two perfluorinated membranes (Nafion 117 and 112) and one hydrocarbon-based membrane [Tokuyama C0011: thickness = 29 μm, proton conductivity (25 °C) = 0.038 S cm^{-1}], purchased from Du Pont and Tokuyama, respectively.

2.2. Characterization and measurements

^{1}H NMR experiments were performed on a Bruker Avance DPX 300 spectrometer at room temperature. Bidirectional permeability measurements were conducted using a home-made diffusion cell consisting of two reservoirs, as depicted in Fig. 1. Membranes were placed between two teflon gaskets with a transporting area of 4 cm^2 bisecting MeOH reservoirs (corresponding to anode sides of DMFCs) and D_2O reservoirs (corresponding to cathode sides of DMFCs). Internal volume of each reservoir was 35 ml.

Permeability was calculated using the following equation describing the relation between liquid concentrations and elapsed times [18,19]:

$$P = \left(\frac{\Delta C_B}{\Delta t}\right)\left(\frac{1}{C_{Ai}}\right)\left(\frac{L}{A}\right)V_B \quad (1)$$

where P is a liquid permeability of a membrane, $\Delta C_B/\Delta t$ is the slope of the molar concentration variation of a liquid as a function of time in the diffused reservoir, C_{Ai} is the initial

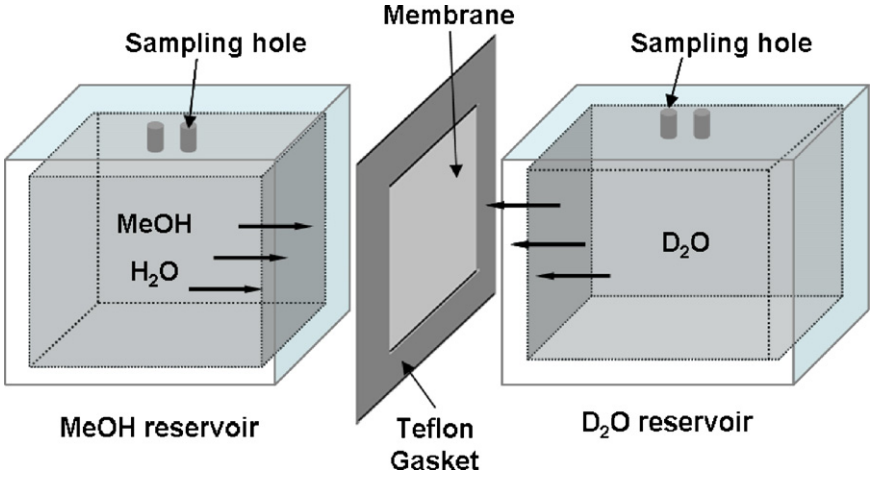

Fig. 1. Schematic diagram representing a home-made diffusion test cell fitted with a proton exchange membrane. The MeOH reservoir contained CH_3OH/H_2O (3 M/48.4 M) and the D_2O reservoir retained D_2O (50 M). Internal volume of each reservoir was 35 ml.

concentration of a liquid in the diffusing reservoir, L and A are the thickness in fully hydrated state and the area of a membrane (4 cm^2), respectively. V_B is the inner volume of the diffused reservoir (35 ml). Methanol, water and D_2O permeability could be estimated using Eq. (1).

Samples (100 μL) retrieved from reservoirs were mixed with a pyridine/DMSO-d_6 solvent (596 mg) of the mass ratio of 0.31/19.8. Pyridine was selected as an external standard for ^1H NMR spectra, because pyridine is dissolved completely in the liquids and a small amount of pyridine shows strong aromatic proton peaks. Furthermore, the characteristic peaks of pyridine (around 7–9 ppm) are not overlapped with those of methanol, water, D_2O and DMSO-d_6.

To verify the permeability obtained with ^1H NMR method, the methanol permeability was re-measured with an ATAGO RX-5000α refractometer which was calibrated with designated MeOH aqueous solutions (1 M, 2 M, 3 M, 5 M, and 10 M). For the RI method, deionized water instead of D_2O was used for the cathode reservoir.

Swelling ratio measurements of membranes in MeOH aqueous solution or deionized water were performed as follows. The membranes were dried under high vacuum at 110 °C for 12 h. After drying, the length, width and thickness of the membranes were measured and, then, immersed in 3 M MeOH aqueous solution or deionized water at room temperature. The sizes (length, width and thickness) of the swollen membranes were re-measured after removal of liquids from membrane surfaces. Swelling ratio of each membrane (%) was calculated using the size variation of the membrane in wet and dried states.

3. Results and discussions

D_2O has a deuterium isotope, the same element with different neutrons, in its molecule. The differences between D_2O and H_2O would be degree of hydrogen bonding, reflective index, etc. Barring the hydrogen-bonding-related properties, D_2O and H_2O exhibit the same physical properties such as melting points and boiling points. In an article related to D_2O and H_2O [17], authors explained that polyethylene oxide (PEO) standard in D_2O showed 3.9% reduction in intrinsic viscosity compared to that in H_2O due to the decrease in the polymer's hydrodynamic volume in D_2O. For size-exclusion chromatography (SEC) calibration curve with polyethylene glycol (PEG) and PEO standards, a slight increase in the elution volumes of the polymers was reported in the D_2O mobile phase. The authors elucidated that the polymers in D_2O have a slightly smaller hydrodynamic volume, but the solvent effects on the hydrodynamic volume of polymers are very small and cannot be seen well visually in the plots. For the measurement of water transport through membranes in this work, the term regarding hydrogen bonding of H_2O needs to be included. The discrepancy of D_2O and H_2O, however, is so small that the term is negligible, as explained in Ref. [17]. Therefore, we inferred from the SEC results that D_2O can be used as the cathodic water for the bidirectional permeability measurements. In addition to the inference, we assume that concentration gradients force the liquids (methanol, water and D_2O) to diffuse through membranes. Consequently, transport behaviors or permeability of membranes can be estimated with Eq. (1) under the conditions as described in Section 2.

3.1. Estimation of bidirectional permeability using ^1H NMR intensity

Permeability values of methanol and water can be determined through the material balance obtained as follows:

The relation between methanol, water and D_2O in MeOH reservoir can be expressed as follows, derived from the constitutive reactions, Eqs. (3)–(5), under a few assumptions:

$$l\mathrm{CH_3OH} + m\mathrm{H_2O} + n\mathrm{D_2O} \rightleftarrows (l-2n)\mathrm{CH_3OH} + (m+n)\mathrm{H_2O} + 2n\mathrm{CH_3OD} \quad (2)$$

where l, m and n represent the molar coefficients of CH_3OH, H_2O and the diffused D_2O in MeOH reservoirs, respectively.

$$l\mathrm{CH_3OH} + n\mathrm{D_2O} \rightarrow (l-p)\mathrm{CH_3OH} + (n-p)\mathrm{D_2O} + p\mathrm{CH_3OD} + p\mathrm{HDO} \quad (3)$$

$$m\mathrm{H_2O} + (n-p)\mathrm{D_2O} \rightarrow (m-n+p)\mathrm{H_2O} + 2(n-p)\mathrm{HDO} \quad (4)$$

$$(l-p)\mathrm{CH_3OH} + p\mathrm{HDO} + 2(n-p)\mathrm{HDO} \rightarrow (l-2n)\mathrm{CH_3OH} + (2n-p)\mathrm{CH_3OD} + (2n-p)\mathrm{H_2O} \quad (5)$$

Assuming that l and m are much higher than n ($l, m \gg n$) and p mole D_2O in the n mole D_2O react with CH_3OH, Eqs. (3)–(5) become simplified and combination of Eqs. (3)–(5) yields Eq. (2).

Eq. (6) concerning the reaction between CH_3OH, H_2O and D_2O in D_2O reservoirs can also be derived from the constitutive reactions, Eqs. (7)–(9), under a few assumptions:

$$x\mathrm{D_2O} + y\mathrm{CH_3OH} + z\mathrm{H_2O} \rightleftarrows (x-y-z+\alpha)\mathrm{D_2O} + y\mathrm{CH_3OD} + (y+2z-2\alpha)\mathrm{HDO} + \alpha\mathrm{H_2O} \quad (6)$$

where x, y, z, and α represent the molar coefficients of D_2O, CH_3OH diffused from MeOH reservoir, H_2O diffused from MeOH reservoir and H_2O formed by the reaction between HDOs in the D_2O reservoirs, respectively.

As the D_2O amounts in D_2O reservoirs are much higher than those of methanol and water, the coefficients of CH_3OH, H_2O and D_2O become $x \gg y, z$. Then, Eqs. (7)–(9) yield Eq. (6).

$$x\mathrm{D_2O} + y\mathrm{CH_3OH} \rightarrow (x-y)\mathrm{D_2O} + y\mathrm{CH_3OD} + y\mathrm{HDO} \quad (7)$$

As given in Eq. (7), if all the CH_3OH diffused in D_2O reservoirs are transformed into CH_3OD by reacting with D_2O in D_2O reservoirs, the H_2O diffused to D_2O reservoirs, then, will react

with D_2O as follows:

$$(x-y)D_2O + zH_2O \rightarrow (x-y-z)D_2O + 2zHDO \quad (8)$$

Eq. (8) is also based on the assumption that all H_2O diffused through membranes into D_2O reservoirs transforms into HDO after reaction with D_2O:

$$yHDO + 2zHDO \rightarrow (y + 2z - 2\alpha)HDO + \alpha H_2O + \alpha D_2O \quad (9)$$

The HDO will form α mole water and D_2O, when the HDOs from Eqs. (8) and (9) react with each other, as shown in Eq. (9). Finally, we can derive the overall reaction, Eq. (6), in the D_2O reservoirs by combining Eqs. (7)–(9).

3.1.1. Estimation of methanol, water and D_2O concentration in MeOH reservoirs using ^1H NMR spectrum

Fig. 2(a) presents a ^1H NMR spectrum of a sample retrieved from MeOH reservoir at 1320 s. Nafion 117 was placed between the two reservoirs. CH_3OH has three methyl protons (CH_3) and one hydroxyl proton (OH), whose peaks appeared at 3.17 ppm and 4.45 ppm, respectively. If CH_3OH reacts with D_2O to form CH_3OD, the peak ratio of methyl protons to hydroxyl protons will deviate from 3:1. The deviation reflects the D_2O amount diffused from cathodes (back-diffusion), and the diffused D_2O amount can be determined by the decreased peak area of hydroxyl protons divided by two, because one D_2O molecule reacts with two hydroxyl protons of CH_3OHs via a substitution reaction between deuteriums and hydroxyl protons.

3.1.2. Estimation of methanol, water and D_2O concentration in D_2O reservoirs using ^1H NMR spectrum

The methanol amounts diffused from MeOH reservoir could be determined by the peak areas of methyl protons. Fig. 2(b) presents a ^1H NMR spectrum of a sample retrieved from D_2O reservoir at 1320 s. The H_2O amount diffused from MeOH reservoir was also calculated with the proton peak area (H_2O) at 3.88 ppm, after subtracting the hydroxyl proton area of CH_3OH from the proton peak area of H_2O, because the peak area at 3.88 ppm included the hydroxyl protons of CH_3OH. Based on the peak assignment, the concentration variation of each solvent could be determined with the peak intensity with respect to time, as given in Fig. 2(c).

3.2. Water diffusion behaviors from MeOH reservoirs to D_2O reservoirs

Fig. 3 represents water diffusion behaviors through membranes from MeOH reservoirs (corresponding to anode sides of DMFCs) to D_2O reservoirs (corresponding to cathode sides of DMFCs). As given in Fig. 3, water transports were affected by the thickness and the chemical structures of membranes, showing the order of Nafion 112 ≫ Tokuyama C0011 > Nafion 117. Water transport behaviors of two perfluorinated membranes (Nafion 112 and 117) indicate that the water diffusion was affected by the thickness of membranes, while the diffusion behaviors of Nafion 112 and Tokuyama C0011 suggest that the

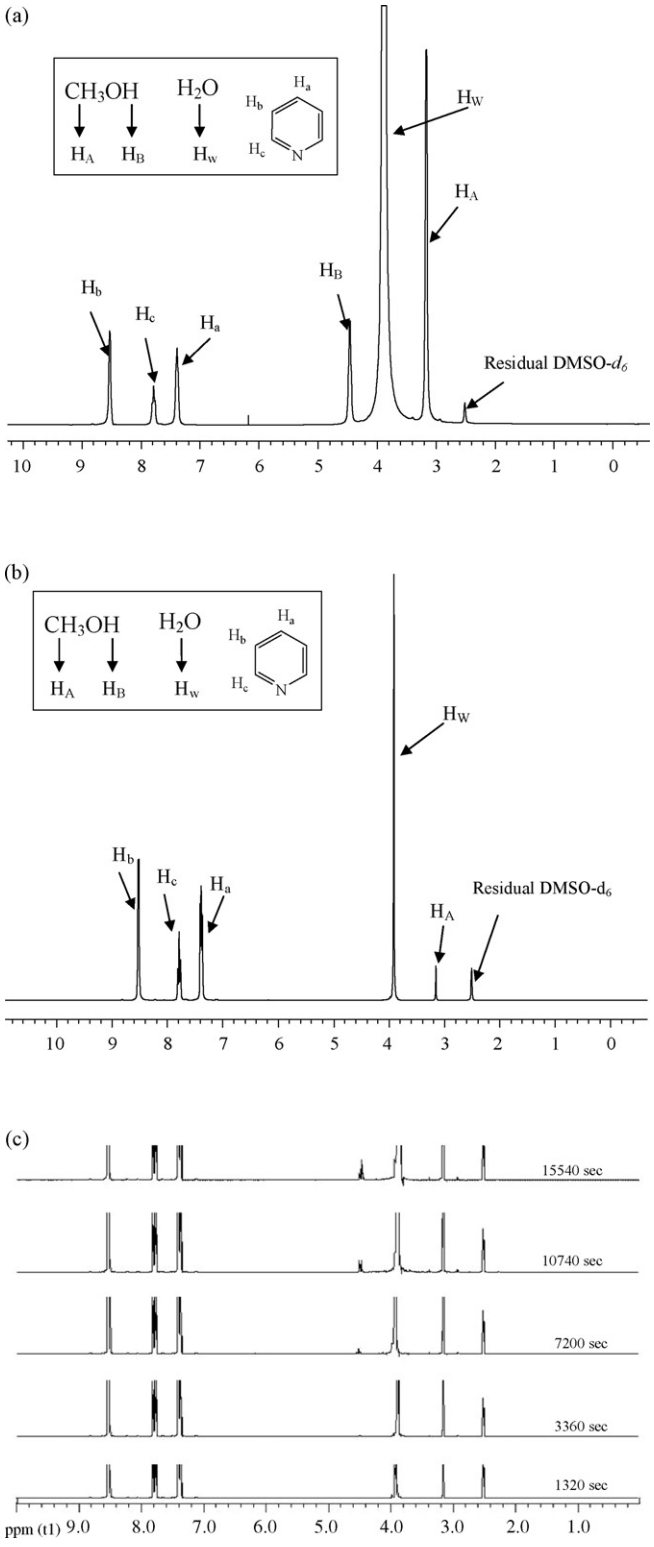

Fig. 2. ^1H NMR spectra of retrieved samples and assignments of solvents: (a) presents the ^1H NMR spectrum of a sample retrieved from the MeOH reservoir at 1320 s, fitted with Nafion 117, (b) exhibits the ^1H NMR spectrum of a sample retrieved from the D_2O reservoir at 1320 s and (c) shows the ^1H NMR spectra of samples retrieved from the D_2O reservoir with respect to time.

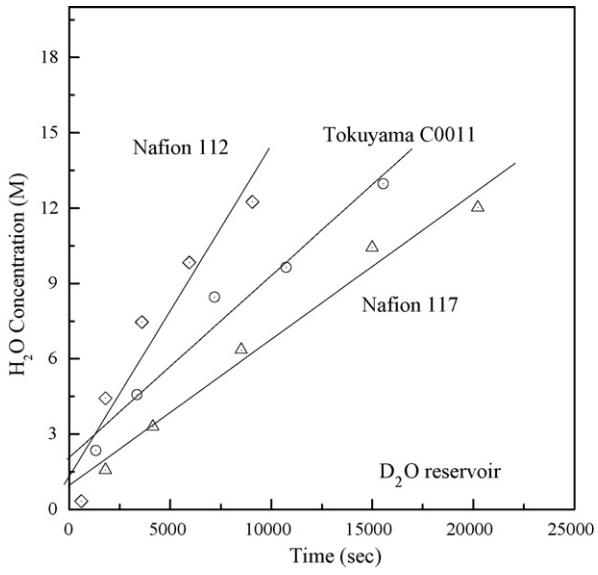

Fig. 3. Molar concentrations of water diffused through membranes with respect to time. Samples were withdrawn from D_2O reservoirs.

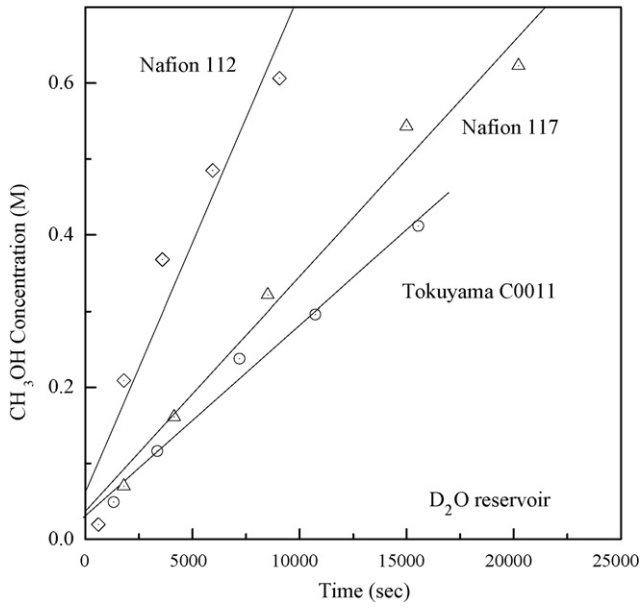

Fig. 4. Molar concentrations of methanol diffused through membranes as a function of time. Samples were collected from D_2O reservoirs, and the solid lines were obtained by fitting the data using OriginPro 7.5.

chemical structures of membranes had an inevitable influence on the diffusions, because Tokuyama C0011 had the thinnest thickness of the membranes (refer Table 1).

3.3. Methanol diffusion behaviors from MeOH reservoirs to D_2O reservoirs

Fig. 4 represents methanol diffusion behaviors through membranes from MeOH reservoirs. Methanol transports also showed the dependence on the thickness and chemical structures of membranes, showing the order of Nafion 112 > Nafion 117 > Tokuyama C0011. Thick membranes exhibited low levels of methanol transportion, as can be seen from transport traces of Nafion 112 and 117. On the other hand, methanol transports had slightly different behaviors from the water transports. The transports of Nafion 117 and Tokuyama C0011 suggest that the chemical structures of membranes had more dominant effect on methanol transports than the thickness of membranes, because Tokuyama C0011 had the thinnest thickness of the membranes. For explaining methanol transport behaviors, swelling ratios of membranes were measured at room temperature, as given in Table 1. The swelling ratios in water and 3 M MeOH aqueous solution appeared as follows: Nafion 117 (41.8%) > Tokuyama C0011 (39.2%) > Nafion 112 (36.8%) in deionized water; Nafion 117 (53.6%) ≈ Nafion 112 (53%) > Tokuyama C0011 (41.2%) in 3 M MeOH aqueous solution. The swelling ratios elucidate that the hydrocarbon is less swollen than Nafion in the methanol solution and the methanol transport behaviors are related to the polarity of solvents, because methanol makes membranes highly swollen, compared to water.

3.4. Molar ratios of methanol to water transported to D_2O reservoirs

Molar transport ratios of methanol to water would provide useful information on interpretation of membrane properties and DMFC operations. As given in Fig. 5, Nafion 112 had the highest molar methanol/water ratio among the membranes, and Nafion 117 also had a higher ratio than the thin hydrocarbon membrane, Tokuyama C0011. The ratio illustrates that Nafion membranes had high methanol permeability, compared to Tokuyama C0011, and the permeability was increased as the thickness of Nafion membrane decreased. The molar MeOH/water ratio of Tokuyama C0011 accords with the report on the low methanol crossover behavior of hydrocarbon membranes [16].

Table 1
Swelling ratios of membranes in water and 3 M MeOH aqueous solution

Membrane	Thickness in dry state (μm)	Expansion (%) in deionized water						Expansion (%) in 3 M MeOH aqueous solution					
		1 h			24 h			1 h			24 h		
		Thickness	Area	Volume	Thickness	Area	Volume	Thickness	Area	Volume	Thickness	Area	Volume
Tokuyama C0011	29	14.3	13.6	29.8	17.9	18.1	39.2	17.9	14.0	34.3	21.4	16.3	41.2
Nafion 117	175	16.0	15.2	33.6	16.6	21.7	41.8	17.2	25.4	46.9	17.8	30.5	53.6
Nafion 112	51	9.8	14.1	25.3	11.8	22.4	36.8	13.7	23.3	40.2	17.6	30.1	53.0

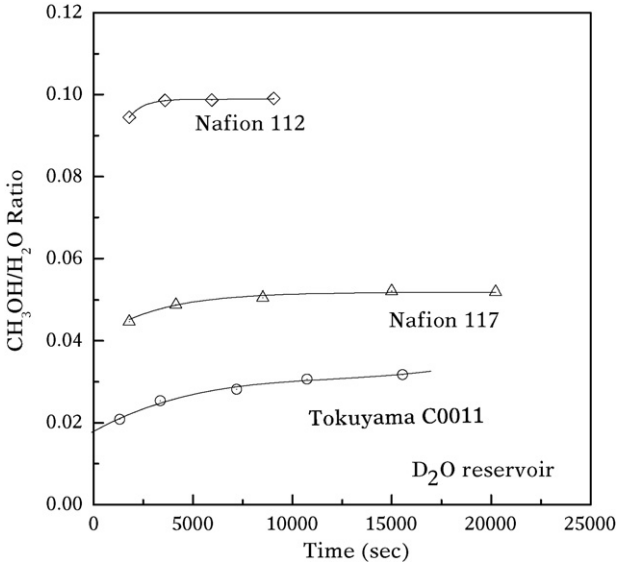

Fig. 5. Variations of molar concentration ratios of methanol to water in D_2O reservoirs as a function of time.

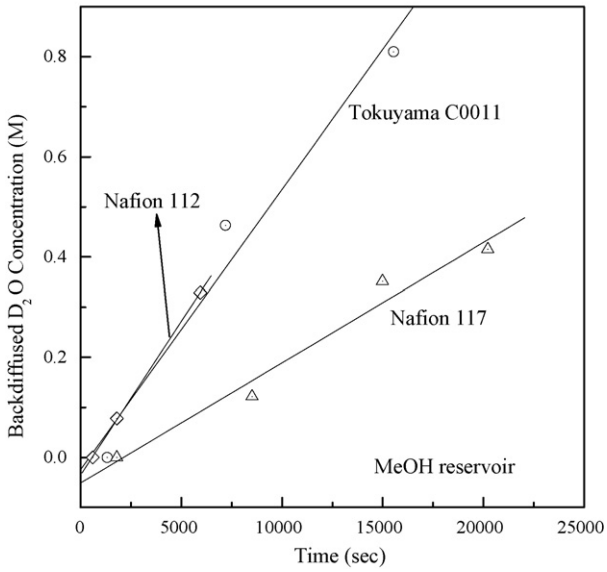

Fig. 6. Back-diffused D_2O concentration variations with respect to time in MeOH reservoirs.

3.5. Reverse-direction diffusion behaviors (back-diffusion behaviors)

Another issue of this paper is to estimate reverse-direction diffusion behaviors of membranes, back-diffusions. Fig. 6 presents the back-diffusion behaviors through membranes. The D_2O diffused to MeOH reservoirs from D_2O reservoirs (from cathodes to anodes) was mainly affected by the thickness of membranes, because thin membranes regardless of chemical structures, Nafion 112 and Tokuyama C0011, had high increase rates, compared to that of Nafion 117. However, the back-diffusion transports [D_2O diffusion from the D_2O reservoirs (cathodes) to MeOH reservoirs (anodes)] were far less in the amount than the water transports [water diffusion from MeOH reservoirs (anodes) to the D_2O reservoirs (cathodes)], exhibiting that the transport proportions of D_2O to H_2O were 6.13% for Tokuyama, 4.15% for Nafion 117, and 4.65% for Nafion 112.

3.6. Permeability determination of membranes

As slopes of molar concentrations against times are key data to calculate the permeability of membranes, the slopes need to be determined. Based on the data of Figs. 3–6, the slopes of solvents were estimated by fitting the data with OrginPro 7.5. Table 2 shows the values determined with the fitting results.

Table 3 presents the permeability values of methanol, water, and D_2O through membranes, calculated with the slope values of Table 2 and Eq. (1). Although Tokuyama 0011 has the thinnest thickness of the membranes, the hydrocarbon membrane exhibited the lowest methanol permeability value, indicating that the methanol permeability was strongly affected by the chemical structures of membranes rather than the thickness of membranes. Furthermore, the methanol permeability values of membranes were nearly the same as those reported in other articles [20]. This indicates that the ^1H NMR method had a considerable reliability in the calculation of permeability. Table 3 also provides information on water transport and back-diffusion of membranes. For water and D_2O transports, the hydrocarbon membrane exhibited the lowest permeability values among the membranes.

Although the permeability values determined with ^1H NMR had similar values reported in other papers, the values needed to be verified with other measurement methods. We selected a reflective index method, which shows reliable data within designated concentrations of methanol. Fig. 7 and Table 4 present the diffusion behaviors of methanol and the methanol permeability values of membranes determined with a RI method, respectively. Since D_2O would affect the reflective index values of methanol aqueous solutions [21], the D_2O in D_2O reservoir was replaced with deionized water, and then we determined the MeOH permeability values using the slopes

Table 2
Slope values presenting molar concentration variations against time. The slopes were determined by fitting data of Figs. 3, 4 and 6

Membrane	D_2O reservoir (cathode side)			MeOH reservoir (anode side)			Ratio of D_2O /H_2O[b]
	CH_3OH (M s^{-1})	H_2O (M s^{-1})	D_2O (M s^{-1})	CH_3OH[a] (M s^{-1})	H_2O[a] (M s^{-1})	D_2O (M s^{-1})	
Tokuyama C0011	2.79×10^{-5}	9.12×10^{-4}	N.A.	-2.51×10^{-5}	-6.65×10^{-4}	5.59×10^{-5}	0.061/1
Nafion 117	3.09×10^{-5}	5.81×10^{-4}	N.A.	-1.60×10^{-5}	-3.14×10^{-4}	2.41×10^{-5}	0.042/1
Nafion 112	6.56×10^{-5}	0.00132	N.A.	-2.05×10^{-4}	−0.00357	6.14×10^{-5}	0.047/1

[a] Slope values were estimated with CH_3OH and H_2O concentrations in MeOH reservoir, and the values present the decreasing rates of CH_3OH and H_2O.
[b] Molar concentration ratios of D_2O diffused into MeOH reservoirs to H_2O diffused into D_2O reservoirs.

Table 3
Methanol, water, and D_2O permeability of membranes, calculated using Eq. (1) and the slope values of Table 1

Membrane	Permeability of CH_3OH ($cm^2\ s^{-1}$)	Permeability of H_2O ($cm^2\ s^{-1}$)	Permeability of D_2O ($cm^2\ s^{-1}$)	Permeability ratio of D_2O/H_2O
Tokuyama C0011	2.77×10^{-7}	5.60×10^{-7}	3.33×10^{-8}	0.060/1
Nafion 117	1.97×10^{-6}	2.30×10^{-6}	9.24×10^{-8}	0.040/1
Nafion 112	1.24×10^{-6}	1.55×10^{-6}	6.98×10^{-8}	0.045/1

Concentrations of liquids: H_2O, 48.4 M; CH_3OH, 3 M; D_2O, 50 M.

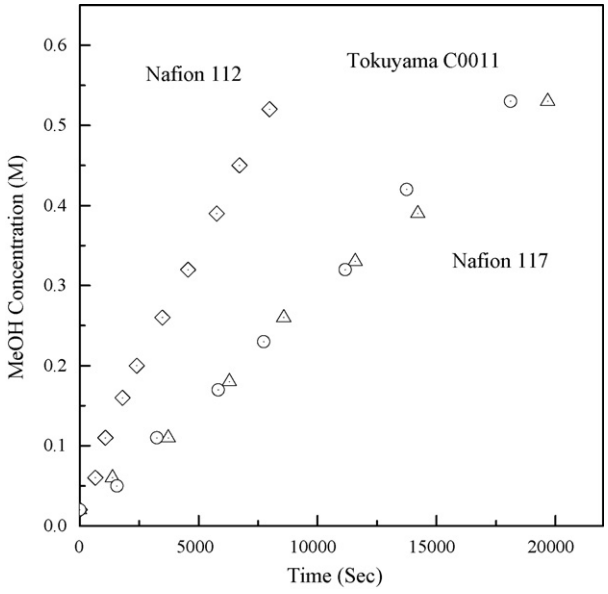

Fig. 7. Methanol diffusion behaviors of membranes with respect to time. The methanol concentrations of samples were estimated with a RI method.

Table 4
Methanol permeability of membranes measured with a RI method

Membrane	Permeability of CH_3OH ($cm^2\ s^{-1}$)	Slope ($M\ s^{-1}$)
Tokuyama C0011	2.85×10^{-7}	2.87×10^{-5}
Nafion 117	1.66×10^{-6}	2.61×10^{-5}
Nafion 112	1.11×10^{-6}	6.18×10^{-5}

of Fig. 7 and Eq. (1). The methanol permeability values were as follows: $2.85 \times 10^{-7}\ cm^2\ s^{-1}$ for Tokuyama C0011, $1.66 \times 10^{-6}\ cm^2\ s^{-1}$ for Nafion 117, $1.11 \times 10^{-6}\ cm^2\ s^{-1}$ for Nafion 112. The permeability values estimated from a RI method exhibited nearly the same results as those estimated with the ^1H NMR method. The permeability with the RI method supports the reliability of the ^1H NMR method.

4. Conclusions

Bidirectional permeabilities of membranes were evaluated by measuring the amount of liquid, methanol and water transports from MeOH reservoirs to D_2O reservoirs (the cathode-directed transport) and D_2O transports from D_2O reservoirs to MeOH reservoirs (the reverse-direction transport), with ^1H NMR spectra. Water transport was affected by thickness and chemical structure of membranes, and methanol had slightly different transport behaviors, depending on the polarity of solvents which affected the swelling ratio of membranes. Another issue of this paper, the reverse-direction diffusion behaviors of membranes (back-diffusions) were determined with the D_2O amounts transported through membranes, exhibiting 4.15–6.13% compared to the transported water amounts. Bidirectional permeabilities of membranes, including back-diffusions, were simultaneously determined with a ^1H NMR technique and we think that this technique can be applicable to other membranes.

References

[1] K.D. Kreuer, J. Membr. Sci. 185 (2001) 29–39.
[2] S.S. Sandhu, R.O. Crowther, J.P. Fellner, Electrochim. Acta 50 (2005) 3985–3991.
[3] R. O'Hayre, S.-W. Cha, W. Colella, F.B. Prinz, Fuel Cell Fundamentals, John Wiley & Sons, 2006, p. 137.
[4] J. Zhang, Y. Wang, Fuel Cells 4 (2004) 90–95.
[5] J. Benziger, J. Nehlsen, D. Blackwell, T. Brennan, J. Itescu, J. Membr. Sci. 261 (2005) 98–106.
[6] A. Heinzel, V.M. Barragán, J. Power Sources 84 (1999) 70–74.
[7] M. Saito, S. Tsuzuki, K. Hayamizu, T. Okada, J. Phys. Chem. B 110 (2006) 24410–24417.
[8] A.S. Aricò, V. Baglio, V. Antonucci, I. Nicotera, C. Oliviero, L. Coppola, P.L. Antonucci, J. Membr. Sci. 270 (2006) 221–227.
[9] J. Cruickshank, K. Scott, J. Power Sources 70 (1998) 40–47.
[10] E. Kjeang, J. Goldak, M.R. Golriz, J. Gu, D. James, K. Kordesch, Fuel Cells 5 (2005) 486–498.
[11] K. Scott, W.M. Taama, P. Argyropoulos, J. Membr. Sci. 171 (2000) 119–130.
[12] T.A. Zawodzinski Jr., M. Neeman, L.O. Sillerud, S. Cottesfeld, J. Phys. Chem. 95 (1991) 6040–6044.
[13] C. Xu, T.S. Zhao, J. Power Sources 168 (2007) 143–153.
[14] T.V. Nguyena, N. Vanderborgh, J. Membr. Sci. 143 (1998) 235–248.
[15] K.A. Mauritz, R.B. Moore, Chem. Rev. 104 (2004) 4535–4585.
[16] M.A. Hickner, H. Ghassemi, Y.S. Kim, B.R. Einsla, J.E. McGrath, Chem. Rev. 104 (2004) 4587–4612.
[17] J.M. Erdner, H.G. Barth, J.P. Foley, W.G. Payne, J. Chromatogr. A 1129 (2006) 41–46.
[18] V. Tricoli, J. Electrochem. Soc. 145 (1998) 3798–3801.
[19] B.S. Pivovar, Y. Wang, E.L. Cussler, J. Membr. Sci. 154 (1999) 155–162.
[20] B. Liu, G.P. Robertson, D.-S. Kim, M.D. Guiver, W. Hu, Z. Jiang, Macromolecules 40 (2007) 1934–1944.
[21] Y.P. Carignan, E.V. Turngren, J. Appl. Polym. Sci. 15 (1971) 1521–1525.